Use of Geomorphological expert knowledge in indirect landslide hazard assessment

C.J. VAN WESTEN, N. RENGERS and R. SOETERS
International Institute for Aerospace Survey and Earth Sciences, ITC, PO Box 6, 7500 AA Enschede, The Netherlands.

Abstract.
The objective of this paper is to evaluate the importance of geomorphological expert knowledge in the generation of landslide susceptibility maps, using GIS supported indirect bivariate statistical analysis. For a test area in the Alpago region in Italy a dataset was generated at scale 1:5000, based on geomorphological mapping. Detailed geomorphological maps were generated, with legends at different levels of complexity. Other factor maps, that were considered relevant for the assessment of landslide hazard were also collected, such as structural geology, bedrock, slope classes, land use, distance from streams, roads and houses. The weights of evidence method was used to generate statistically derived weights for all classes of the factor maps. On the basis of these weights, the most relevant maps were selected for the combination into landslide susceptibility maps. Six different combinations of factor maps were evaluated, with varying geomorphological input. Success rates were used to classify the weight maps into three landslide susceptibility classes. The resulting six maps were compared with a direct hazard map. The analysis indicated that the use of detailed geomorphological factor maps raised the overall accuracy of the hazard maps from 52 to 76 percent. However, even with the use of a detailed geomorphological factor map, the difference with the separately prepared direct hazard map is still significant, due to the generalisations that are inherent to the bivariate statistical analysis technique.

Key words: landslide hazard, indirect mapping methods, weights of evidence modelling, GIS, geomorphology

1. Introduction

Many different types of landslide hazard zonation techniques have been developed over the last decades (Soeters and Van Westen, 1996). Generally speaking these techniques can be subdivided into direct and indirect methods. In direct hazard mapping the geomorphologist, based on his experience and knowledge of the terrain conditions determines the degree of hazard directly. Indirect hazard mapping uses either statistical models or deterministic models to predict landslide prone areas, based on information obtained from the interrelation between landscape factors and the landslide distribution. The increasing popularity of Geographic Information Systems for landslide hazard assessment over the last decades has lead to a majority of studies on indirect hazard mapping approaches. GIS is very suitable for indirect landslide hazard mapping, in which all possible causative terrain parameters are combined with a landslide distribution map, using data-integration techniques (Van Westen, 1993; Bonham-Carter, 1994; Chung et al, 1995). One of the simplest methods, the landslide information value method (Yin and Yan, 1988) is defined as the logarithm of the ratio between the density of landslides in a class over the density of landslides for the whole area. Chung and Fabbri (1993, 1999) developed statistical procedures under the name of predictive modelling, applying favourability functions on individual parameters. Using these statistical methods, terrain units or grid cells are transformed to new values representing the degree of probability, certainty, belief or plausibility that the respective terrain units or grid cells may contain or can be expected to be subject to a particular landslide in the future.

The use of indirect methods such as bivariate statistics has a number of drawbacks. One of these is the tendency to simplify the factors that cause landslides, by taking only those that can be relatively easily mapped in an area, such as slope angle or lithology. Another problem is related to generalisation, assuming that landslides happen under the same combination of factors throughout the study area. The third problem is related to the fact that each landslide type will have its own set of causal factors, and should be analysed individually (Kojima *et al*., 2000). A fourth problem is the lack of expert opinion, which is common in the application of these methods. For most geomorphologists it is very difficult to formulate the expert evaluation that they applied in the direct hazard mapping, into clear decision rules.

This study intends to contribute to bridging the gap between the direct and indirect landslide hazard zonation methods, by evaluating the importance of geomorphological expert knowledge in the generation of landslide susceptibility maps, using GIS supported indirect bivariate statistical analysis.

2. The study area

The study was carried out on a test site in the Alpago basin, located to the East of Belluno, Italy (see figure 1). The study area, with a size of 20.8 km², consists of two watersheds: the Borsoia watershed to the South and the Boccolana watershed in the North. The northeastern part of the area is formed by a steep mountain ridge, consisting of limestone, that rises up to more than 2000 meters. The western part is underlain by Flysch, and has a more gentle, undulating morphology with an average altitude around 1200 meters. A detailed geological description of the area is given by Mantovani *et al*. (1976).

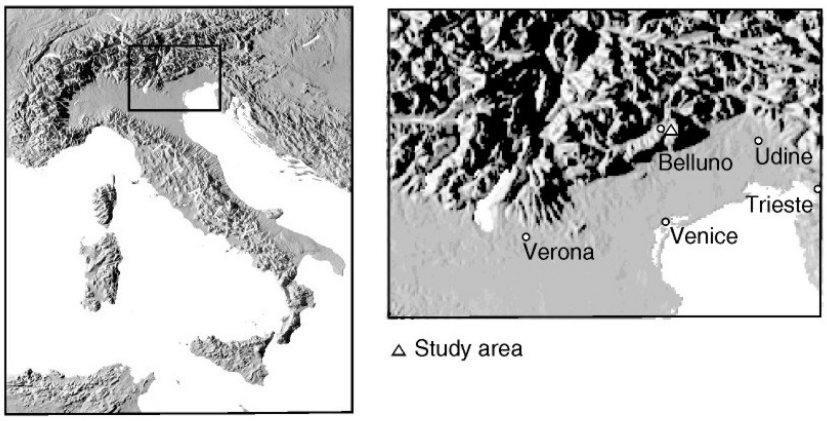

Figure 1: Location of the study area.

The Geomorphology of the area is dominated by glacial and denudational landforms. Many different glacial depositional and erosional landforms give evidence of a complex deglaciation history, where the regional Piave glacier interacted with the local Borsoia glacier. An overview of the various deglaciation phases is given by Van Westen *et al*. (2000b). The area shows evidences of a history of active massmovements. Many landslides are found, varying in type, activity and age. On the basis-of geomorphological indicators, such as glacial reworking, a number of the landslides located at higher altitudes were interpreted as pre-glacial (Van Westen *et al*., 2000b), where others are interpreted as being from late glacial, early Holocene or Late Holocene times.

3. Direct hazard mapping

For the study area a detailed geomorphological hazard map was constructed, based on a detailed photo-interpretation, performed with airphotos from 1954 to 1980, having a scale of 1:10.000 to 1:30.000. A detailed field check was made and the resulting geomorphological units were drawn on 1:5.000 scale topographical maps.

The hazard type and degree of each individual polygon was evaluated on the basis of geomorphological criteria, such as the presence of evidences of mass movement activity (e.g. scarps, cracks, tilted trees, moved blocks etc), the freshness and relative age of these features, the location near other polygons that might cause danger (e.g. location below a scarp, or above a retrogressive landslide), or the presence of other factors that might cause slope instability (such as slope deposits, subglacial tills, steep slopes, water stagnation etc).
The following five layers of geomorphological information were digitised with the Geographic Information System ILWIS, and stored in the database of the Alpago area:

- *Main geomorphological unit map (layer 1)*, consisting of 425 different polygons in 52 legend classes, which show information on the genesis and material types, and the chronological information (see table 2).
- *Geomorphological sub-unit map (layer 2)*, consisting of 1774 different polygons in 81 legend classes, which contain detailed descriptions on each slope segment.

Geomorphological sub-units are the smallest sections of the terrain that can be presented on a large-scale map. A geomorphological sub-unit consists of one landform, for which the genesis, together with morphographical characteristics is given.

- *Process map (layer 3)*, in which all units with mass movement processes are stored. This map consists of 409 polygons with unique identifiers. The map is linked to an attribute table, which contains information on the mass movement type, the dimensions of the mass movement phenomena, and the main cause for the occurrence.
- *Surface material map (layer 4)*, consisting of 185 polygons with 21 legend units. There may be some overlap with layer 1, where the material type forms one of the criteria for defining main units. However, the polygons in this layer contain a full coverage of material types.
- *Geomorphological hazard map (layer 5)*, in which all information is stored on the classification related to mass movement hazards. This map contains 241 polygons with unique identifiers. For each hazard polygon the deciding factors for the hazard classification were recorded in a database. For about 90% of the hazard polygons, the geomorphological information contained in the main- and sub-unit layers were sufficient for providing these decision criteria. Besides of the hazard class, also the type of hazard was indicated (small rockfall, large rockfall, landslides, flowslides, flows, erosion, flooding and snow avalanches). The legend was kept simple, using only three levels of hazard (high, moderate, and low).

For this study the process map was simplified to a map displaying only the active landslides in the area (see figure 2). This map was used in the indirect hazard assessment as the evidence map. Also the geomorphological hazard map was modified so that it only indicated the information related to mass movements of slide and flow type. Other processes, such as rockfall were not left out, since they occur under a different set of conditions and would have to be analyzed separately.

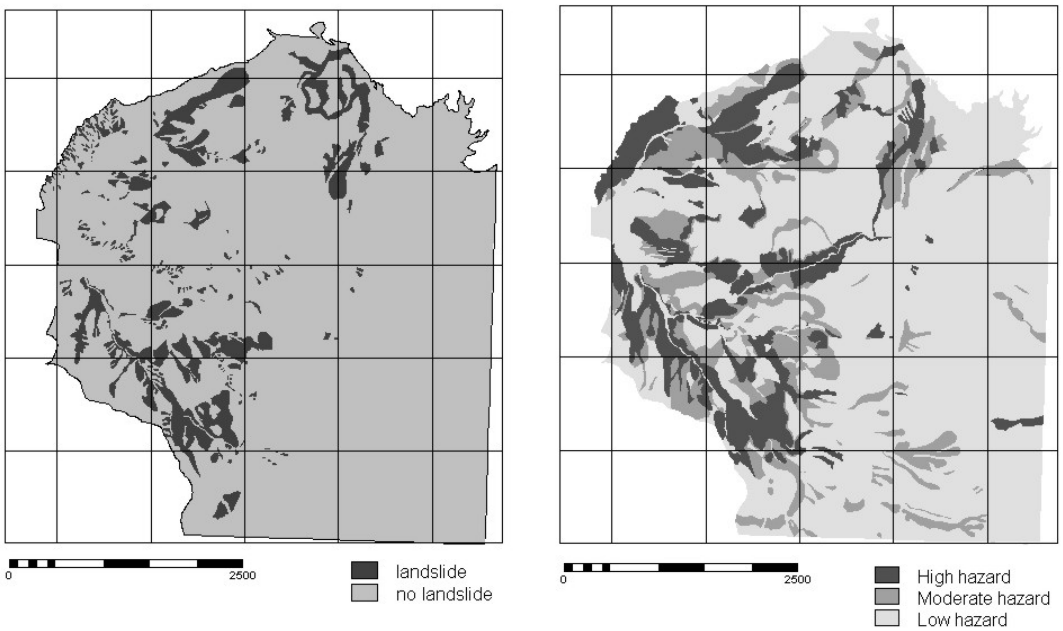

Figure 2. Left: Simplified process map used for the indirect hazard assessment, showing only the location of active landslides. Right: Simplified geomorphological hazard map, based on direct field evaluation, which was used for comparison with the statistically derived hazard maps.

4. Indirect hazard mapping

In this study the weights of evidence method (Bonham-Carter, 1994) was selected for the indirect hazard assessment. In this method positive and negative weights (W_i^+ and W_i^-) are used, which are defined as:

$$W_i^+ = \log_e \frac{P\{B_i|S\}}{P\{B_i|\overline{S}\}} \qquad \text{[eq. 1]}$$

and

$$W_i^- = \log_e \frac{P\{\overline{B_i}|S\}}{P\{\overline{B_i}|\overline{S}\}} \qquad \text{[eq. 2]}$$

where,
B_i is the class of a factor map, and
S is landslide

W_i^+ is used for those pixels where the class of a factor map is present, and the value indicates the importance of the class for predicting landslides. If the value is negative the class can be used to indicate where landslides are not likely, and when it is positive it is used to indicate where landslide are more likely to occur. W_i^- is used to evaluate the importance of the absence of the class to predict where landslides can be expected.

In GIS the weights of evidence method can be implemented rather easily. For the combination of one class of a factor map and the landslide map, there are four possible combinations, of which the frequency, expressed as number of pixels, can be calculated by overlaying the maps (see table 1).

			B_i : Class of factor map	
			(present)	(absent)
S: Landslides	Present	1	$Npix_1$	$Npix_2$
	Absent	0	$Npix_3$	$Npix_4$

Table 1: Four possible combinations of a class of a factor map and a landslide map

Based on equations [1] and [2] the weights of evidence can be written in numbers of pixels as follows:

$$W_i^+ = \log_e \frac{\frac{Npix_1}{Npix_1 + Npix_2}}{\frac{Npix_3}{Npix_3 + Npix_4}} \qquad \text{[eq. 3]}$$

and

$$W_i^- = \log_e \frac{\frac{Npix_2}{Npix_1 + Npix_2}}{\frac{Npix_4}{Npix_3 + Npix_4}} \qquad \text{[eq. 4]}$$

Although the method was originally designed for the use of binary maps, it is also possible to calculate in ILWIS the weights for all classes in a multi-class map simultaneously.

5. Analysis of the factor maps

For the weights of evidence modelling the following factor maps were generated (see table 2 and 3)

- Bedrock map, indicating the main geological units in the areas;

- Structural geological map, showing the location of dip-slopes and face-slopes, as they were expected to have a relation with landslides;
- Surficial materials, showing the types of quaternary deposits. This information was derived from the geomorphological mapping;
- Land use, prepared by fieldwork, photo-interpretation and the existing information on the 1:5000 scale maps.
- Slope angles, in classes of 10 degrees. This map was generated from the Digital Elevation Model. The DEM was made through the interpolation of contour lines from 4 digitised 1:5.000 toposheets, with contour interval of 2.5 meters;
- Distance from roads. This map was made by applying a buffer to the road network, which was classified into two classes (< 25 meter from the road, and 25-50 meters from the road). This factor map was generated to test the hypothesis that landslides may be more frequent along roads, due to cutting of slopes and inappropriate drainage from the road;
- Distance from streams. Also this map was generated using a buffer, in this case around the stream network, and the same two distance classes were used as for the roads. The hypothesis that was checked was the possible higher landslide frequency along streams, due to undercutting.
- Main geomorphological units, and Geomorphological subunits, which were mentioned earlier.

All maps were stored in raster format (1909 rows, 1772 columns) with a pixelsize of 3 meters. The factor maps were all combined with the map of active landslide for the calculation of the weights. The calculation procedure was written in the form of a script file, consisting of a series of GIS commands. The script makes use of variables for carrying out the same set of operations for all factor maps selected. For each of the classes of the factor maps positive and negative weights were calculated. Adding the positive weight of the class itself and the negative weight of the other classes of the same multi-class map gave a final weight for each class. The resulting weights, as shown in table 2 and 3, were used to make a selection of the most relevant classes and factor maps.

As can be concluded from tables 2 and 3, some of the factor maps showed hardly any relation with the occurrence of landslides, as evidenced by weights close to 0. For example, the slope classes showed values that oscillate around zero, without any extreme positive or negative values. This indicates that slope is not a very good predicting factor in this study area. The distance from roads and the distance from streams were both also not very important, as the weights were not very pronounced. With respect to the bedrock types, the analysis proved that the presence of calcareous rocks is a clear indicator for the absence of landslides, as this factor had the highest negative weight (-8.5), followed by the presence of rockfall (-7.9) and scree (-4.9). This is also due to the fact that all active rockfall processes were removed from the training data set, and were not included in the analysis.

The geomorphological units (see table 3) had much more pronounced weights than the other factor maps (see table 2), as can be seen from the very high negative and high positive weights. The geomorphological units dealing with the various landslide phases (pre-glacial, early postglacial, sub-recent Holocene and recent), obviously have a high relation with the occurrence of active landslides, either as new ones or as reactivations of old landslide complexes. The geomorphological sub-units showed an even higher relation with maximum weights up to +14. The results are not shown here, due to the extensive legend of the geomorphological sub-unit map. However, the geomorphological sub-units were mapped in such a detailed way that the high positive weights nearly completely coincide with the landslide pattern, and therefore is not considered very useful for the prediction of new landslides.

5. Selection of scenarios

Based on the weights presented in the previous section, a number of combinations of factor maps were selected, in order to test their predictive power. The following combinations were selected for further analysis:

- Map 1. Only the factors bedrock type and slope classes were used, since in many landslide hazard studies these are the two factor maps that are used (e.g. Brabb, 1984).
- Map 2. Weights were used from the following factor maps: structural geology, bedrock type, slope classes, land use and distance from drainage. Those factors were used that were most important, and had the highest weights, to test how good the prediction would be if geomorphological input data is not used.

- Map 3. For constructing this map the same factor maps were used as in the previous case, with addition of the surface material map.
- Map 4. This map was made using the same combination of factors as for map 3, but with the addition of the main geomorphological units.
- Map 5. Here, instead of the main geomorphological units, the geomorphological sub-units were used as factor map, combined with the same factors as for map 3.
- Map 6: Weights are only used from the geomorphological maps (mainunit and subunits), without any other factor map.

Map	Class	Weight
Structural geology	Dipslope	1.514627
	Faceslope	0.406060
Surficial materials	ablation moraine	-2.997582
	ablation moraine & flysch	0.669640
	Alluvial	-4.365125
	cemented scree	1.092740
	Colluvium	-5.234163
	fluvio-glacial	-5.229821
	landslide material	1.563517
	landslide material from flysch	1.231779
	landslide material from moraine	1.424658
	landslide material from moraine&flysch	1.987710
	landslide material from scree&flysch	-1.546675
	landslide material from subglacial till	4.367070
	landslide material from weathered flysch	1.868644
	Moraine	0.359593
	Rockfall	-7.857759
	Scree	-4.932881
	subglacial till	0.798947
Bedrock	calcareous rocks	-8.518484
	flysch	1.272424
Land use	bare	1.322403
	bare&shrubs	0.931164
	forest	0.029859
	forest(young)	-1.325931
	grass	-0.961017
	grass&agric	-1.882213
	grass(swampy)	2.076442
	settlement	-0.103685
	shrubs	0.829082
Slope	0 -10 degrees	-0.413311
	10 - 20 degrees	0.093273
	20 -30 degrees	0.048432
	30 -40 degrees	-0.029504
	40 -50 degrees	0.254631
	50 -60 degrees	0.241418
	60 -70 degrees	-0.392213
	70-80 degrees	-2.433674
Distance from roads	<25 m from road	-0.271342
	25-50 m from road	-0.094518
Distance from streams	< 25 m from drainage	0.739747
	25-50 m from drainage	0.541094

Table 2: Weights for classes of the non-geomorphological factor maps, as calculated by the weights of evidence modelling.

Code	Geomorphological group	Geomorphological unit	Weight
111	Landforms related to the PIAVE glacier	Ice-marginal complexes related to maximum glaciation	-8.497910
112		Ice-marginal complexes related to the contact of the Piave glacier with local glaciers	-6.763876
113		Complex of glacially eroded slopes and levels (partly ice-marginal) related to recession phases	-2.137759
114		Fluvioglacial fans	-5.617430
115		Subglacial till levels with flucioglacial reworking	-0.211804
116		Glacially eroded slopes	-1.085356
117		Glacially eroded pre-glacial landslide niches	0.633573
121	Landforms related to the Borsoia glacier	Ice-marginal complexes related to various recession phases	-9.586844
122		Glacially eroded slopes	-2.618129
131	Landforms related to minor local glaciers	Morainic complex of maximum glaciation	-5.844747
132		Cirque	-8.092548
133		Glacially eroded valley	-8.987155
134		Fluvio-glacial fans	-6.464728
211	Denudational plateaus	In calcareous rocks with minor kartification processes)	-8.495727
221	Denudational slopes	In calcareous rocks	-10.736714
222		In flysch	-1.161314
223		In morainic material	0.385285
231	Accumulation of slope deposits	Scree slopes	-7.304544
232		Rockfall deposits	-7.900251
233		Colluvial slopes	-7.759841
241	Denudational niches	In calcareous rocks	-8.362938
242		In flysch rocks	0.723635
243		In moraininc materials	2.007113
251	Denudational valleys	In calcareous rocks	-5.806453
252		In flysch rocks	1.163205
253		In morainic materials	-0.270045
254		In mass movement materials	0.788522
311	Pre-glacial landslides	Collapsed cemented scree slope complex, with clear landslide blocks	1.464854
312		Collapsed cemented scree slope comples, with chaotic landslide mass	-7.147784
321	Early postglacial landslides	Dipslope related	0.133656
322		Failure of subglacial till level	1.487659
323		Flow-mass, caused by loading of scree material on top of flysch	1.380578
324		Rotational landslide in moraine covered flysch	-1.829337
325		Landslide in ablation moraine	-1.562957
330	Sub-recent Holocene landslides	Reactivation of older landslide: dipslope related	0.673034
331		Reactivation of older landslide: failure of subglacial till level	-0.187895
332		Reactivation of older landslide: contact of moraine and flysch	2.918090
333		Reactivation of older landslide: related to other situations	0.640132
334		New landslide: dipslope related	3.159034
335		New landslide: faceslope related	2.517143
336		New landslide: failure of subglacial till	2.423631
337		New landslide: contact of moraine and flysch	1.840670
338		New landslide: due to stream undercutting	-1.584268
339		New landslide: related to other situation	2.199059
341	Recent landslides	Reactivation of older landslide: dipslope related	8.602759
342		Reactivation of older landslide: contact of moraine and flysch	5.131376
344		New landslide: dipslope related	9.437425
345		New landslide: faceslope related	2.797559
346		New landslide: contact of moraine and flysch	8.483261
347		New landslide: due to stream undercutting	10.475438
410	Floodplain and terraces	Of Borsoia and Boccolana rivers	-5.178649
420	Alluvial fans	In Borsoia glacial valley	-7.964455

Table 3: Legend of the main geomorphological units, and the weights, as calculated by the weights of evidence modelling.

For each of the 6 map combinations, the factor maps were reclassified with the weights from the attribute tables, and the weight maps were combined into a single map. These resulting 6 maps were again combined with the original landslide map, in order to calculate the success rate. The success rate (see figure 3) shows how much percentage of the landslides occur in the pixels with the highest values in the weight map. For this purpose the pixels in the weight map were ordered according to their weights (from high to low) and classified into classes of 5 %. This reclassified map was combined with the landslide map, and the percentage of the total amount of landslides was calculated for each class.

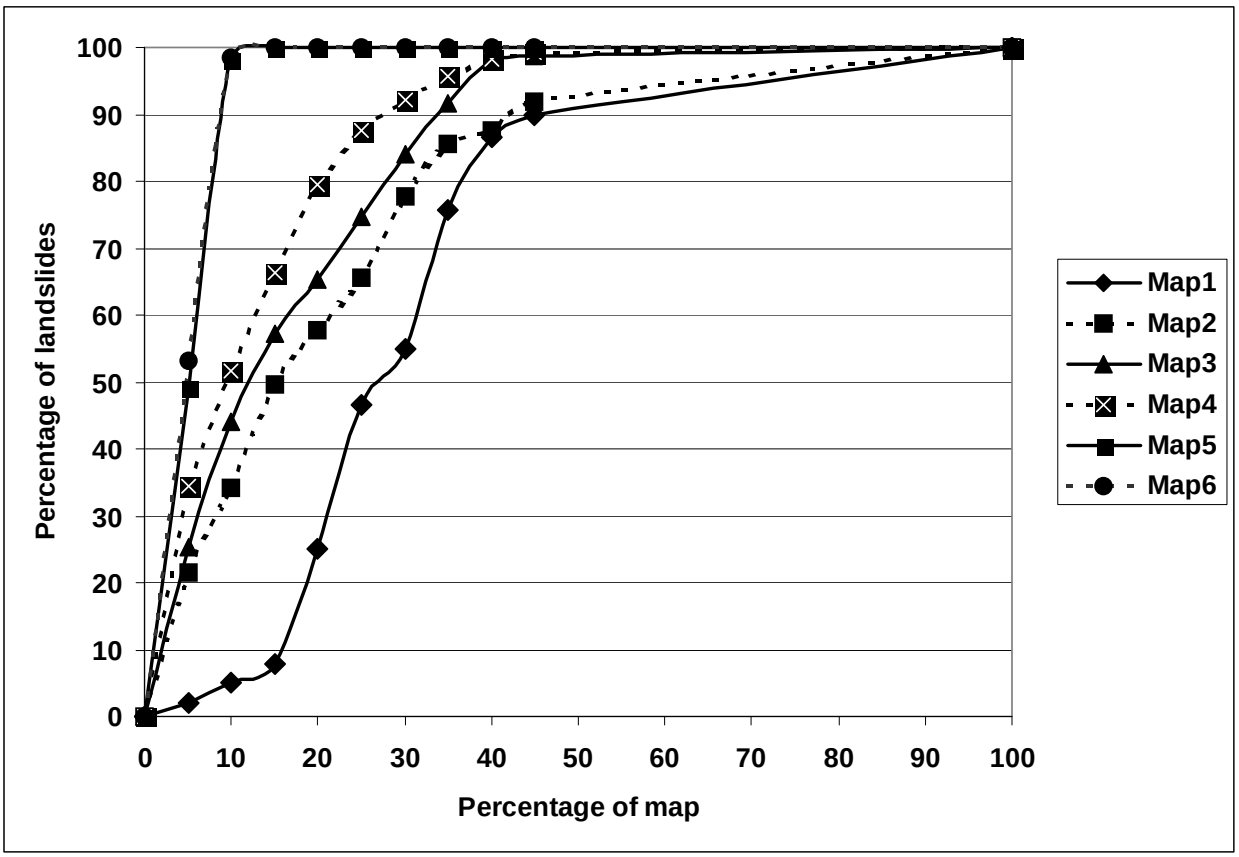

Figure 3: Success rates calculated for the 6 different scenarios. See text for explanation.

As can be seen from figure 3, the success rate improves from map 1 to map 6. So the more detailed geomorphological information is used, the better is the prediction capacity. Since no multi-temporal landslide data set was available, it was not possible to calculate the prediction rate. However, the success rate by itself is also a useful indicator for the quality of the map, although it merely shows how good the resulting weight scores can explain the input landslide pattern that was used to calculate them.

It is clear from figure 3 that in the Alpago area the combination of only slope and geology will not lead to an acceptable result. It is also interesting to observe that the use of geomorphological information improves the success rate considerably. The use of the geomorphological main-units is preferred over the more detailed sub-units, because the latter ones will nearly lead to a resulting map that is almost similar as the input landslide pattern, and therefore has no large prediction power in areas which are not covered by landslides yet.

The success rate curves were also used to classify the 6 weight maps into three classes (high, moderate and low hazard), by taking a fixed percentage of landslides, and using the corresponding weight value as threshold. For the high hazard class the threshold was set at 75 percent of all landslides. For the moderate hazard class this was done at 15 percent of the landslides (90% of the total), and for the low hazard class at the remaining 10 percent. The six classified maps are shown in figure 4.

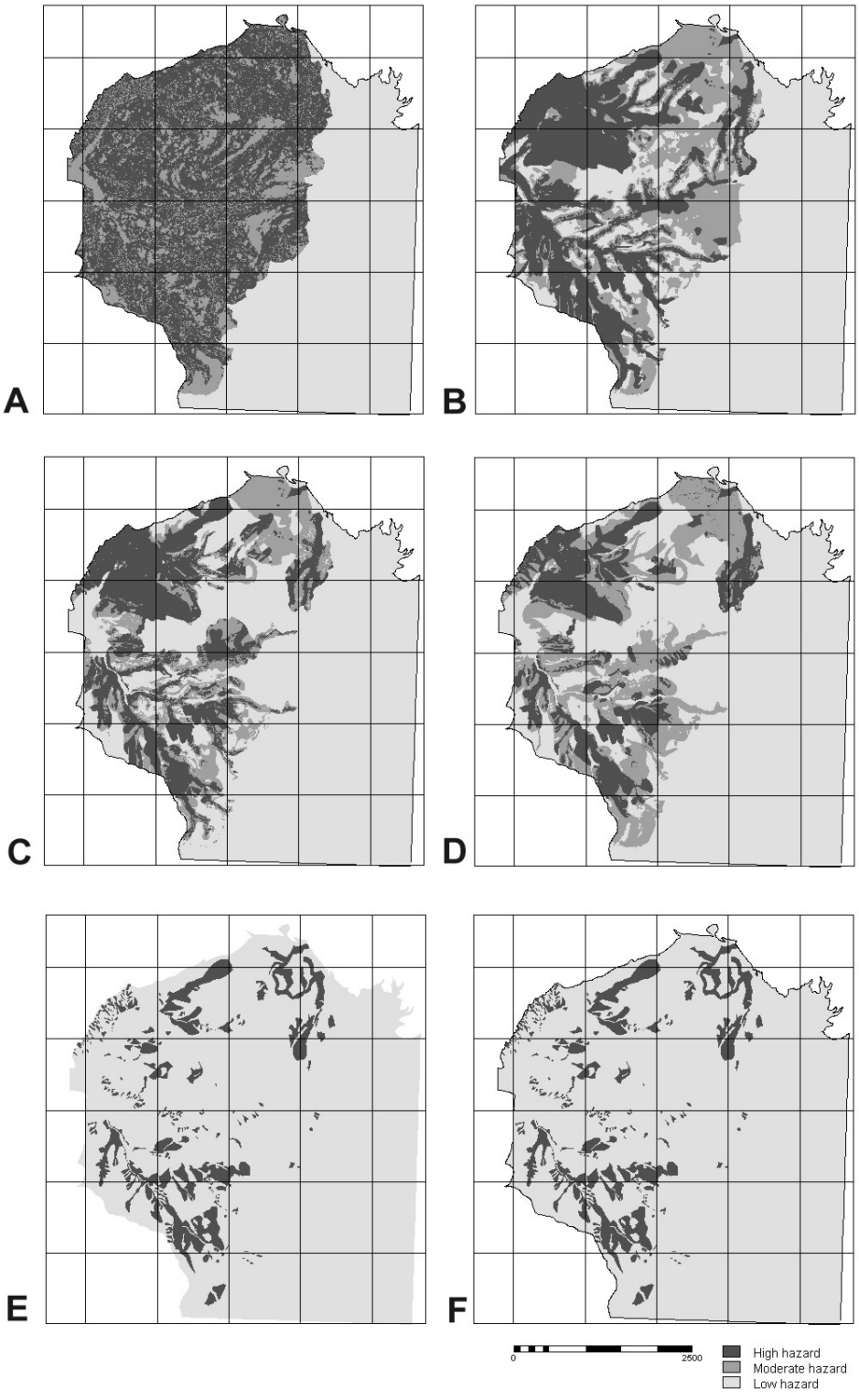

Figure 4: The classified hazard maps for the six different map combinations. A = Map 1, B = Map 2, C= Map 3, D= Map4 , E= Map5 and F= Map 6.See text for explanation.

The spatial pattern of the 6 maps is quite different, although all of them have classified the limestone area in the east as low hazards. From Map 1 to Map 6, with increasing importance

of geomorphological information, the size of the high and moderate hazard areas is decreasing. The hazard map made only by combining slope classes and lithology (Figure 4 A) gives a very poor result, with a randomly distributed high hazard class. The hazard maps, which are based on the very detailed geomorphological information (figure 4 E and F), show a near complete overlap with the original landslide map, with very small or even absent moderate classes.

6. Comparison of direct and indirect hazard maps

Finally, the accuracy of the six classified hazard maps (see figure 4), made from different combinations of factor maps, were compared with the direct hazard map (see figure 2). This was done by calculating a confusion matrix for each of the six situations, followed by a calculation of the accuracy. It was assumed that the direct hazard map represent the "true" situation, since it was carefully prepared by experts, based on many field observations (Van Westen *et al*., 2000a). The results are shown in table 4.

	INDIRECT HAZARD MAP 1				
DIRECT HAZARD MAP		Low	Moderate	High	Reliability
	Low	886689	268517	444431	0.55
	Moderate	81139	55214	218777	0.16
	High	13022	86912	247897	0.71
	Percent of map	42.62	17.83	39.55	
	Accuracy	0.90	0.13	0.27	
	INDIRECT HAZARD MAP 2				
DIRECT HAZARD MAP		Low	Moderate	High	
	Low	1087324	172624	339689	0.68
	Moderate	133950	54649	166531	0.15
	High	29139	32428	286264	0.82
	Percent of map	54.32	11.27	34.40	
	Accuracy	0.87	0.21	0.36	
	INDIRECT HAZARD MAP 3				
DIRECT HAZARD MAP		Low	Moderate	High	
	Low	1330828	37745	159459	0.84
	Moderate	131363	48180	152188	0.19
	High	33287	25080	264710	0.76
	Percent of map	64.96	4.82	30.22	
	Accuracy	0.89	0.43	0.46	
	INDIRECT HAZARD MAP 4				
DIRECT HAZARD MAP		Low	Moderate	High	
	Low	1336484	103694	159459	0.84
	Moderate	135042	67900	152188	0.19
	High	24696	58424	264710	0.76
	Percent of map	65.00	9.99	25.02	
	Accuracy	0.89	0.30	0.46	
	INDIRECT HAZARD MAP 5				
DIRECT HAZARD MAP		Low	Moderate	High	
	Low	1577744	0	21765	0.99
	Moderate	321158	0	33956	0.00
	High	173242	0	174529	0.50
	Percent of map	90.00	0	10.00	
	Accuracy	0.76	?	0.76	
	INDIRECT HAZARD MAP 6				
DIRECT HAZARD MAP		Low	Moderate	High	
	Low	1578498	0	22082	0.99
	Moderate	321219	0	33895	0.00
	High	172851	0	174921	0.50
	Percent of map	89.99	0	10.01	
	Accuracy	0.76	?	0.76	

Table 4: Confusion matrices for the six indirect hazard maps, as compared to the classes of the direct hazard map.

The overall accuracy of the six hazard maps was calculated by dividing the number of pixels that were correctly classified (the diagonals in table 4) over the total number of pixels in the study area. The result showed the following overall accuracy values for map1 to map 6: 51 %, 62 %, 72 %, 76 % and 76% percent for map 6.

5. Discussion and Conclusions

The analysis indicated that the use of detailed geomorphological factor maps raised the overall accuracy of the hazard maps from 51 to 76 percent. The accuracy of the high hazard classes only demonstrates this even more. The range is there from 27 percent for map 1 to 76 percent for map 6. It is clear from these results that in the Alpago area the combination of only slope and geology will not lead to an acceptable result, because the lithology is rather homogeneous and landslides occur on different slope angles . The use of other factor maps, such as structural geology and landuse increases the accuracy, but the main step of improvement in this area is made by the inclusion of geomorphological information.

One aspect, which was clearly demonstrated in this study, was that every study area has its own particular set of factors for the prediction of landslides. For example, the slope map and lithology map in this area turned out to be of little use, whereas in other areas these may be the main controlling factors.

From the results it is also clear that the use of the very detailed geomorphological sub-units will lead to an unacceptable limitation of the high hazard areas, nearly overlapping with the input landslide pattern. The resulting hazard maps (map5 and 6) therefore are not considered to very useful for the prediction of new landslides. The use of the geomorphological main-units is considered to be the best approach in this area.

However, even with the use of geomorphological factor maps, the difference with the direct hazard map is still significant. The maximum accuracy reached with the indirect methods does not exceed 76 percent. This is due to a number of factors. One of the most important ones is the generalisation that is inherent to the bivariate statistical analysis technique, assuming that landslides are controlled by the same combination of factors throughout the area. The direct geomorphological mapping, on the other hand, is able to evaluate subtle changes in the landslide controlling factors, and make specific judgements for each particular site. The direct hazard map also includes factors that are difficult to include within the bivariate statistical method, such as the areas above or below active scarps, where landslides may extend in the future.

The bivariate statistical method gives a satisfactory combination of the (subjective) professional geared direct mapping and the (objective) data driven analytical capabilities of a GIS. The main advantage of bivariate statistical procedures is that the determination of factors or combinations of factors used in the assessment is determined by the professional, who executes the analysis. This enables the introduction of expert opinion into the process. The methodology asks for a careful confrontation of the hazard prediction with the "real world" and an adaptation of decision rules there where differences are observed, this mostly on experience driven criteria. Bivariate statistics are a useful tool in the assessment of landslide hazards, but can best be used as a supporting tool for a geomorphologist, to make quantitative estimations of the importance of the various factors involved. The actual generation of the hazard maps is best done by knowledge driven methods, such as multi-class index overlaying or fuzzy logic methods.

References

Bonham-Carter, G.F.(1994) Geographic Information Systems for Geoscientists; modelling with GIS. Computer methods in Geosciences, Vol. 13, Pergamon Press, pp. 398

Brabb, E.E. (1984) Innovative approaches to landslide hazard and risk mapping. Proceedings 4th International Symposium on Landslides, Toronto, Canada, Vol. 1, pp 307-324.

Chung, C.F. and Fabbri, A.G. (1993)The representation of geoscience information for data integration. Nonrenewable Resources, Vol. 2:2, pp.122-139

Chung, C.J., Fabbri, A. and Van Westen, C.J. (1995). Multivariate regression analysis for landslide hazard zonation. A. Carrara and F. Guzetti (eds). Geographical Information Systems in Assessing Natural Hazards. Kluwer, pp 107-133.

Chung, C.F. and Fabbri, A.G., 1999. Probabilistic prediction models for landslide hazard mapping, Photogrammetric Engineering & Remote Sensing, Vol.65, No.12, pp.1389-1399.

Mantovani, F. Panizza, M., Semenza E. and Piacente, S. (1976). L'Alpago (Prealpi Bellunesi). Geologia, Geomorfologia, Nivopluviometria. Boll. Soc. Geol. It. 95, pp 1589-1656.

Kojima, H. , Chung, C.J. and Van Westen,C.J. (2000) Strategy on the landslide type analysis based on the expert knowledge and the quantitative prediction model. ISPRS congress 2000. International Archives of Photogrammetry and Remote Sensing, Vol. XXXIII, Part B7, pp. 701 - 708.

Soeters, R. and Van Westen C.J. (1996). Slope Instability Recognition, Analysis and Zonation. In: Turner, A.K. and Schuster, R.L. (eds). Landslides, investigation and mitigation. Transportation Research Board, National Research Council, Special Report 247, National Academy Press, Washington D.C., U.S.A., p 129-177.

Van Westen, C.J. (1993). Application of Geographic Information Systems to Landslide Hazard Zonation. Ph-D Dissertation Technical University Delft. ITC-Publication Number 15, ITC, Enschede, The Netherlands, 245 pp.

Van Westen, C.J., Soeters, R. and Sijmons, K. (2000) Digital Geomorphological landslide hazard mapping of the Alpago area, Italy. International Journal of Applied Earth Observation and Geoinformation. Volume 2, Issue 1, pp. 51-59

Van Westen, C.J. Seijmonsbergen, A.C. and Mantovani, F. (2000) Comparing landslide hazard maps. Natural Hazards 20, pp.137-158

Yin, K.J. and Yan, T.Z. (1988) Statistical prediction model for slope instability of metamorphosed rocks. Proceedings 5 th. International Symposium on Landslides, Lausanne, Switserland, Vol.2 : 1269-1272

List of tables:

List of figures: